Johnson, C. K. (1976) ORTEPII, Report ORNL-5138, Oak Ridge National Laboratory, Oak Ridge, TN.
Kallen, R. G., Korpela, T., Martell, A. E., Matsushima, Y., Metzler, C. M., Metzler, D. E., Morozov, Yu. V., Ralston, I. M., Savin, F. A., Torchinsky, Yu. M., & Ueno, H. (1985) in *Transaminases* (Christen, P., & Metzler, D. E., Eds.) pp 37–108, John Wiley & Sons, New York.
Kamitori, S., Hirotsu, K., Higuchi, T., Kondo, K., Inoue, K., Kuramitsu, S., Kagamiyama, H., Higuchi, Y., Yasuoka, N., Kusunoki, M., & Matsuura, Y. (1987) *J. Biochem. 101*, 813–816.
Kamitori, S., Okamoto, A., Hirotsu, K., Higuchi, T., Kuramitsu, S., Kagamiyama, H., Matsuura, Y., & Katsube, Y. (1990) *J. Biochem. 108*, 175–184.
Kiick, D. M., & Cook, P. F. (1983) *Biochemistry 22*, 375–382.
Kirsch, J. F., Eichele, G., Ford, G. C., Vincent, M. G., Jansonius, J. N., Gehring, H., & Christen, P. (1984) *J. Mol. Biol. 174*, 497–525.
Kondo, K., Wakabayashi, S., & Kagamiyama, H. (1987) *J. Biol. Chem. 262*, 8648–8657.
Kuramitsu, S., Hamaguchi, K., Ogawa, T., & Ogawa, H. (1981) *J. Biochem. 90*, 1033–1045.
Kuramitsu, S., Okuno, S., Ogawa, T., Ogawa, H., & Kagamiyama, H. (1985) *J. Biochem. 97*, 1259–1262.
Kuramitsu, S., Hiromi, K., Hayashi, H., Morino, Y., & Kagamiyama, H. (1990) *Biochemistry 29*, 5469–5476.
McPherson, A. (1982) *Preparation and Analysis of Protein Crystals*, pp 96–97, John Wiley & Sons, New York.
Mehta, P. K., Hale, T. I., & Christen, P. (1989) *Eur. J. Biochem. 186*, 249–253.
Messing, J. (1983) *Methods Enzymol. 101*, 20–78.
Messing, J., Crea, R., & Seeburg, P. H. (1981) *Nucleic Acids Res. 9*, 309–321.
Nakamaye, K. L., & Eckstein, F. (1986) *Nucleic Acids Res. 14*, 9679–9698.
Sung, M.-H. (1989) Ph.D. Thesis, Kyoto University.
Taylor, J. E., Metzler, D. E., & Arnone, A. (1990) *Ann. N.Y. Acad. Sci. 585*, 58–67.
Toney, M. D., & Kirsch, J. F. (1987) *J. Biol. Chem. 262*, 12403–12405.
Velick, S. F., & Vavra, J. (1962) *J. Biol. Chem. 237*, 2109–2122.
Yano, T., Kuramitsu, S., Tanase, S., Morino, Y., Hiromi, K., & Kagamiyama, H. (1991) *J. Biol. Chem.* (in press).

Effects of Point Mutations in a Hinge Region on the Stability, Folding, and Enzymatic Activity of *Escherichia coli* Dihydrofolate Reductase†

Patricia M. Ahrweiler‡ and Carl Frieden*
Department of Biochemistry and Molecular Biophysics, Washington University School of Medicine, St. Louis, Missouri 63110
Received February 28, 1991; Revised Manuscript Received May 13, 1991

ABSTRACT: The role of a hinge region in the folding, stability, and activity of *Escherichia coli* dihydrofolate reductase was investigated with three site-directed mutants at valine-88, the central residue of the hinge. The three mutants, V88A and V88I and a valine-88 deletion, were created to perturb the packing of hydrophobic residues in the interior of a loose turn formed by residues 85–91. Deleting the valine-88 residue destabilized the protein by 2.93 ± 0.6 kcal/mol as determined by equilibrium unfolding transitions in urea monitored by circular dichroism at 20 °C. Substitution of alanine for valine-88 stabilized the protein by −0.20 ± 0.02 kcal/mol, and the isoleucine substitution was mildly destabilizing by 1.73 ± 0.2 kcal/mol. Although there was no clear correlation between side-chain volume and stability, these results suggest that side-chain interactions in the interior of the turn influence the folding and stability of dihydrofolate reductase. The specific activity of the valine deletion mutant was approximately twice that of the wild-type protein while the specific activities of the V88A and V88I proteins were only slightly greater than the wild type. The full time courses of the reactions catalyzed by the mutants were almost identical with that for the wild type, indicating no major changes in the kinetic mechanism. Additionally, the rate constants associated with interconversion between various forms of the apoenzyme were identical for the mutant and wild-type enzymes. The rate constants for refolding transitions were examined by dilution of urea-inactivated protein. While the refolding properties of the V88A mutant were similar to wild type, some rate constants for phases observed in refolding of the valine deletion and the V88I mutant were decreased about 3-fold relative to the wild type. The phase most affected in both these mutants has been previously shown to be related to the formation of the binding site for dihydrofolate during refolding, indicating that the valine-88 residue may be at a region that is involved in bringing preformed elements of secondary structure together to form the dihydrofolate binding pocket.

Dihydrofolate reductase (DHFR, EC 1.5.1.3)[1] from *Escherichia coli* is an ideal candidate for studying the effects of single amino acid replacements on protein folding and stability. It is a small, monomeric protein (17 680 daltons, 159 amino acids) with no prosthetic groups or disulfide bonds. The three-dimensional structure of the binary DHFR–methotrexate complex has been determined to high resolution (1.7 Å) (Bolin et al., 1982; Filman et al., 1982), allowing some structural

† Supported by USPHS Grant DK13332.
* Author to whom correspondence should be addressed.
‡ Present address: Hybritech, Inc., San Diego, CA 92126.

[1] Abbreviations: DHFR, dihydrofolate reductase; MTX, methotrexate; PMSF, phenylmethanesulfonyl fluoride; H_2F, dihydrofolate; H_4F, tetrahydrofolate.

0006-2960/91/0430-7801$02.50/0

interpretation of the effects of single amino acid replacements on folding. The kinetic behavior of DHFR has also been well characterized (Penner & Frieden, 1985, 1987; Fierke et al., 1987), allowing a wide range of experimental characterization of mutant proteins. Finally, the gene for *E. coli* dihydrofolate reductase has been cloned and is available in a high-expression system (Villafranca et al., 1987). The equilibrium and kinetic folding behavior of wild-type DHFR in the presence of urea has been well characterized, and many site-directed mutants of *E. coli* DHFR have been constructed to study α-helix and β-sheet formation (Perry et al., 1987), electrostatic interactions (Perry et al., 1989), and hydrophobic packing effects (Garvey & Matthews, 1989; Garvey et al., 1989), during the folding process.

We became interested in a particular turn region of DHFR as a target for site-directed mutagenesis to study the folding and conformation of DHFR. Residues 85–91 of *E. coli* DHFR form a loose turn that reverses the direction of the α-carbon backbone from α-helix E to β-sheet E (Bolin et al., 1982) and is believed to be part of a hinge region (along with residues 35–38 of an opposing turn in the structure) that separates the molecule into two domainlike structures (Bystroff & Kraut, 1991). The turn was classified as two consecutive type IV β-turns by Bolin et al. (1982), residues 85–88 (C-G-N-V) and residues 88–91 (V-P-E-I). However, the turn protrudes from the protein's surface and resembles ω turns described in detail by Leszczynski and Rose (1987).

The role of turn regions in protein folding is ambiguous. Monte Carlo simulations have indicated that turn regions participate in the early events of protein folding (Skolnick & Kolinski, 1990). Turns have been shown to be expendable (Wallace, 1987) or interchangeable (Hynes et al., 1989) units of secondary structure whose conformation depends upon the local interactions of residues in the loop. However, Alber et al. (1987) found that point mutations that disrupted the hydrogen bonding in an irregular, solvent-exposed loop of T4 lysozyme destabilized the protein toward temperature denaturation. Deletion of two residues from a flexible loop region of human DHFR (Tan et al., 1990) abolished activation by KCl, urea, and organomercurials observed in the wild-type enzyme.

We have constructed three site-directed mutants of *E. coli* DHFR with mutations at valine-88, the central residue in the loose-turn region connecting α-E to β-E. We first deleted valine-88 (ΔV88) and then substituted alanine (V88A) or isoleucine (V88I) at the 88 position. Since an important feature of turn regions is the packing of residues, these substitutions were designed to disrupt the hydrophobic packing of the Cys85, Val88, and Ile91 residues in the loop's interior. It was also anticipated that these mutations could disrupt the loop's function as a mobile or a hinge element in the folding process or produce subtle conformational changes in the native state. In this paper, we report the effects of these point mutations on the stability of the protein toward urea denaturation, the enzymatic activity of the protein, and the rate constants for the kinetic refolding reactions.

Materials and Methods

Plasmid and Mutant Constructions. Vector pMDR was constructed for the mutagenesis experiments by subcloning the *Bam*HI insert containing the DHFR coding sequences of plasmid pTY1 (Villafranca et al., 1982) into the *Bam*HI site of pMOJ3, a pBR322-derived phagemid vector. Single strands from this vector were isolated by infection of the host strain with helper phage. The oligonucleotides used for the mutagenesis were prepared on an Applied Biosystems DNA synthesizer Model 380B, A88 (5′-GCGTGTGGTGACGCCCCAGAAATCATGGTG-3′), I88 (5′-GGCGTGTGGTGACATCCCAGAAATCATGGTG-3′), and ΔV88 (5′-GGCGTGTGGTGAC|CCAGAAATCATGGTG-3′) (substitution nucleotides are shown in boldface print). The valine-88 deletion oligo is designed to "loop out" the 88 codon at the vertical bar separating the two halves of the oligo. The mutagenesis reaction for the valine-88 deletion was performed according to the method of Zoller and Smith (1972), with no selection for mutagenized single strands. The alanine-88 and isoleucine-88 mutants were constructed as above except the mutant strand was synthesized with native T7 DNA polymerase (United States Biochemical) and 5-methyldeoxycytidine triphosphate (d5′MeCTP) was added to the standard deoxynucleotides. The d5′MeCTP renders the mutant strand resistant to a number of restriction enzymes including *Hpa*II, *Msp*I, and *Sau*3A (Vandeyar et al., 1988). The nonmethylated strand of the hemimethylated DNA molecule was nicked with *Sau*3A, and the nicked strand was removed with exonuclease III. The methylated single-stranded mutant DNA was transformed into *E. coli* strain SDM (United States Biochemical), a *mcr*AB$^-$ mutant strain that does not restrict the d5′MeCTP DNA. Cells were made competent by the rubidium chloride method (Maniatis et al., 1982) and did not remain viable when stored at −70 °C.

Transformants were picked onto nitrocellulose filters (Schleicher & Schuell) placed on LB–ampicillin (100 μg/mL) plates in a grid array for low-density colony hybridization screening (Miller, 1977). Cells grown on the nitrocellulose filter were lysed, and the DNA was fixed to the filter by placing the filters "face up" sequentially onto 1–2-mL puddles of (1) 0.5 N NaOH/1.0 M NaCl (2×), (2) 1 M Tris-HCl, pH 7.4 (2×), and (3) 1.5 M NaCl/0.5 M Tris-HCl, pH 7.4 (2×) (arranged on a large piece of Saran wrap taped to the bench top), for 2 min each. The solutions soak through the nitrocellulose membranes and do not disturb the lysed cells on the filters. Excess cellular debris was rinsed from the filters by shaking gently in 1.5 M NaCl/0.5 M Tris-HCl, pH 7.4. The filters were baked at 60–80 °C for 1–3 h and stored wrapped in Saran at 40 °C until use.

Mutant clones were identified by the following procedure. The filters were prehybridized with 4× hybridization buffer (HPB) (1× HPB is 0.5 M NaCl, 0.1 M sodium phosphate, and 6 mM EDTA, pH 7.0) (Cameron et al., 1979), 1% sodium *N*-lauroylsarcosine, and 50 μg/mL salmon testis DNA at 60 °C and then hybridized with the same solution plus 50 pmol of ^{32}P-kinased mutagenic oligonucleotide for 2 h. Filters were washed once at room temperature with 1× HPS and 1% *N*-lauroylsarcosine and then 2 times at 60 °C for 10 min. At this temperature, the mutagenic oligo melts off the wild-type DHFR sequences but remains hybridized to the mutant plasmid DNA, giving a positive signal when exposed to autoradiographic XAR-5 film for 3 h to overnight. Positives were colony-purified and rescreened. Single-strand or plasmid DNA from secondary positives was sequenced with Sequenase (United States Biochemicals Corp.) to verify the correct mutations, and the remaining DHFR coding sequences were then confirmed by dideoxy sequencing.

The mutant plasmids pMDRΔV88, pMDRA88, and pMDRI88 were transformed into strain PA414, a strain of *E. coli* with the *fol* gene deleted (Ahrweiler & Frieden, 1989), for protein expression and purification. The engineered mutation at the valine-88 codon of DHFR-transformed plasmid was reconfirmed before use in protein purification by dideoxy sequencing of plasmid DNA isolated from PA414. The use

of the *fol* deletion strain eliminates the problem of contamination with wild-type DHFR expressed from the chromosomal bacterial gene or loss of the mutant plasmid sequences from recombination with wild-type chromosomal DHFR coding sequences.

Protein Purification. Purification of the mutant DHFR proteins was performed roughly according to the procedures of Baccanari et al. (1975) and Prendergast et al. (1988) for purification of wild-type DHFR. Cell pellets from 200-L fermenter cultures were stored at −70 °C until use. Approximately 300 g of frozen cells was thawed and suspended in 300 mL of ice-cold 40 mM Tris-HCl, pH 8.0, 20 mM EDTA, 1 mM DTE, and 1 mM PMSF. The cell suspension was lysed in a French press cylinder at 2000 psi for 20 s. The lysed cells were centrifuged at 143000*g* for 1 h at 4 °C. The supernatant was decanted, and the pellets were washed with equal volumes of lysis buffer and centrifuged as before. The supernatants were combined and assayed for DHFR activity. The crude lysate was brought to 85% saturation with ultrapure ammonium sulfate (ICN Biochemicals) and centrifuged at 6300*g* for 30 min. The resulting 0–85% ammonium sulfate pellet was resuspended in 5 volumes of 40 mM potassium phosphate, 0.2 M KCl, 2 mM EDTA, 1 mM DTE, and 1 mM PMSF, pH 6.0 (low-salt phosphate buffer), and loaded on an MTX–agarose column (Sigma Chemical Co., St. Louis, MO) equilibrated with the same buffer.

A 3.0 × 10.0 cm MTX–agarose column was used for the V88A and V88I mutant proteins, and a smaller 1.5 × 5.0 cm column was used for the ΔV88 protein since there was approximately 10-fold less activity in the crude lysate. Use of a larger column for the ΔV88 purification resulted in very poor elution and low yields of ΔV88 protein. The column was washed with 20–40 column volumes of the low-salt phosphate buffer and then with 200 mM KH_2PO_4, 1 M KCl, 2 mM EDTA, 1 mM DTE, and 1 mM PMSF, pH 6.0 (high-salt phosphate buffer). The DHFR mutant protein was eluted with high-salt phosphate buffer containing 3 mM folic acid (Sigma), pH 8.0, at a flow rate of 1.0 mL/min. Fractions containing DHFR activity were pooled and dialyzed against 50 mM Tris-HCl, 50 mM KCl, 1 mM DTE, and 1 mM EDTA, pH 7.2, and then loaded onto a DEAE-Sepharose column preequilibrated with the dialysis buffer. The DHFR mutant protein was eluted with a gradient of 50–400 mM KCl in 50 mM Tris-HCl, 1 mM DTE, and 1 mM EDTA, pH 7.2. Fractions with DHFR activity were pooled and concentrated in an Amicon ultrafiltration unit using a YM3 membrane. The concentrated protein was passed over a final 2.0 × 80 cm G-50 column equilibrated in 50 mM Tris-HCl, 50 mM KCl, 1 mM EDTA, and 1 mM DTE, pH 7.2. Fractions with DHFR activity were concentrated to 1–5 mg/mL.

The purity of the protein preparation was assessed by detection of a single band of the correct molecular weight stained with Coomassie blue following SDS–polyacrylamide gel electrophoresis (PAGE). Ultraviolet spectra from 190 to 300 nm were collected to confirm the identity of the protein as homogeneous DHFR, and to confirm the absence of folic acid, nucleic acids, or other contaminants.

Enzymatic Assays and Active-Site Titrations. The DHFR (wild type and mutants) concentrations were determined by methotrexate titrations as previously described (Williams et al., 1979). Specific activities were determined from initial portions of full time course enzymatic assays on an Applied Photophysics stopped-flow spectrophotometer (Model SFMV12). The reaction conditions were 50 mM [bis(2-hydroxyethyl)amino]tris(hydroxymethyl)methane (Bis-Tris), pH 7.2, 50 μM EDTA, 1 mM DTE, 0.050 μM enzyme, 20 μM NADPH (Sigma type III), and 10 μM dihydrofolate [H_2F, prepared from folic acid (Zakrzewski & Sansone, 1971)], 20 °C. The DHFR enzyme was preincubated with the NADPH to avoid nonlinear initial velocities (Penner & Frieden, 1985), and the reaction was followed at 340 nm, using a differential millimolar extinction coefficient of 11.8 cm^{-1} (Stone & Morrison, 1982).

Fluorescence Quenching Experiments. Substrate quenching of the intrinsic fluorescence of the protein was performed under the same buffer conditions as those for enzyme assays using the Applied Photophysic stopped-flow apparatus in the fluorescence mode with a 0.2-cm light path. The excitation wavelength was 285 nm. For H_2F, a 305-nm cutoff filter was used on the emission side while for NADPH a UG1 long-wavelength cutoff filter was used in conjunction with the 305-nm filter.

Equilibrium Unfolding Experiments. Unfolding of the DHFR proteins in urea could be assessed with either fluorescence or circular dichroism spectroscopy. For the wild-type and DV88 mutants, results from fluoresence and circular dichroism were the same, but the fluorescence experiments were more difficult to access because of large slopes of the curves in regions outside the transition area. The equilibrium curves were therefore determined from circular dichroism spectroscopy by measuring the molar ellipticity at 222 nm, a wavelength that is sensitive to the presence of secondary structure in the protein. Each data point for the equilibrium curve consisted of 0.10 mg/mL DHFR protein, 0–6.0 M urea, 20 mM potassium phosphate, pH 7.2, and 0.1 mM EDTA. Samples were allowed to equilibrate 10 min at 20 °C in the water-jacketed cell in the spectrophotometer before data were collected. The ellipticity, θ, was measured on a Jasco J600 spectropolarimeter interfaced with an IBM PS2 Model 50 computer in a 1-mm light path cell by scanning from 210 to 250 nm at a rate of 20 nm/min. Three spectra were collected, averaged, and then smoothed with a 5-nm window. Molar ellipticity (θ) at 222 nm was plotted versus urea concentration to generate the equilibrium curve. Concentrated stock solutions were prepared by dissolving ultrapure urea (ICN Biochemicals) in distilled, deionized water and then deionized by adding 1 g of mixed-bed resin (Bio-Rad AG501-X8) per 150 g of urea and stirring at room temperature for 1 h. The solutions were filtered through a 0.45-μm Millipore membrane. The exact urea concentration was determined with an Abbe refractometer at 25 °C and equations relating refractive index to concentration (Pace, 1986; Santoro & Bolin, 1988). The urea stock solutions were stored at −20 °C until use and were not reused.

The data from the urea-induced equilibrium unfolding curve were fit directly to the equation:

$$\theta = \{(\theta_N + m_N[D]) + (\theta_U + m_U[D]) \times \exp[-(\Delta G^\circ_{H_2O}/RT + m_G[D]/RT)]\}/\{1 + \exp[-(\Delta G^\circ_{H_2O}/RT + m_G[D]/RT)]\} \quad (1)$$

a complete mathematical description of the two-state cooperative unfolding reaction relating θ (ellipticity at 222 nm) and denaturant concentration, [D] (Santoro & Bolin, 1988). A nonlinear least-squares program (SAS Institute, Cary, NC) was used to calculate the parameters θ°_N, θ°_U, m_N, m_U, m_G, and $\Delta G^\circ_{H_2O}$.

The equilibrium constant K_U for unfolding in the presence of urea is obtained directly from the spectroscopic data by

$$K_U = (\theta_N - \theta)/(\theta - \theta_U) \quad (2)$$

where θ is the observed ellipticity and θ_N and θ_U are the values

of ellipticity of the native and unfolded forms, respectively. The θ_N and θ_U values may vary with denaturant concentration according to eq 3 where m_N and slopes of the pre- and post-

$$\theta^\circ_N = \theta_N + m_N[D] \text{ and } \theta^\circ_U = \theta_U + m_U[D] \quad (3)$$

unfolding regions, respectively. The observed equilibrium constants in the unfolding transition region are converted to free energy data (ΔG_{obs}) since $\Delta G_{obs} = -RT \ln K_U$. The free energy of unfolding, ΔG_{obs}, is known to vary linearly with denaturant concentration according to

$$\Delta G_{obs} = \Delta G^\circ_{H_2O} + m_G[D] \quad (4)$$

The values of $\Delta G^\circ_{H_2O}$ (the free energy of the unfolding reaction in the absence of denaturant) and m_G may be calculated from a plot of ΔG_{obs} as a function of denaturant concentration, by extrapolation to zero denaturant concentrations to find the intercept, $\Delta G^\circ_{H_2O}$, and the slope, m_G.

Kinetic Folding Experiments. The refolding reactions were followed by fluorescence changes using the Applied Photophysics stopped-flow spectrophotometer at either 10 or 20 °C. Fluorescence measurements were performed by using an excitation wavelength of 285 nm (2-mm slits) with a 0.2-cm light path collecting the fluorescence signal above 305 nm. The final denaturant concentration was controlled through the use of different size drive syringes to obtain the appropriate dilution from the initial conditions. Protein at 0.1 mg/mL in 20 mM potassium phosphate, pH 7.2, 0.1 mM EDTA, 1 mM DTE, and the initial urea concentration was placed in the smaller syringe. Data were recorded by using a split time base, with 500 points collected over the first few seconds and 500 points collected for the remaining time. The multiexponential fitting program supplied by Applied Photophysics was used to analyze the kinetic data according to the equation:

$$A(t) = \sum A_i \exp(-k_i t) + A_\infty$$

where $A(t)$ is the amplitude of the change at time t, A_∞ is the amplitude at infinite time, A_i is the amplitude at zero time of phase i, and k_i is the rate of phase i. The first 100 ms of the data was not included in the fit because of a mixing artifact of about 30–40 ms. Goodness of fit was assessed by the distribution of residuals about the mean.

While the wild-type and mutant enzymes were found to be free of any major contaminants, such as folate, it is always possible that small amounts remained. As shown elsewhere, however, the presence of substrates during refolding experiments of the type performed here does not affect the rate constants for the refolding process (Frieden, 1990).

Results

Protein Expression and Purification. The yields of mutant DHFR protein expressed from plasmids pMDRΔV88, pMDRV88A, and pMDRV88I in strain PA414 varied. The ΔV88 mutant was poorly expressed, and approximately 0.08 mg of protein was isolated per gram of cell paste. This was 40-fold less than the amount of wtDHFR isolated from HB101.pTY1, a similar vector–strain combination (3.3 mg of DHFR/g of cell paste). Strain PA414 also grew slower when expressing ΔV88 than when expressing the wtDHFR, V88A, or V88I, and reached a lower final optical density at 600 nm. Approximately 0.35 mg of mutant protein/g of cell paste was isolated from both the PA414.pMDRV88A and PA414.pMDRV88I cultures, 10-fold less than wild type. All three mutant DHFR proteins, ΔV88, V88A, and V88I, bound tightly to the MTX–agarose column did not elute with high-salt phosphate buffer, and required the presence of substrate

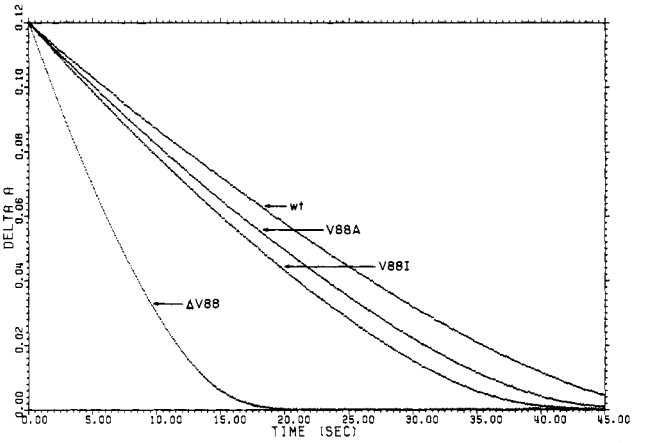

FIGURE 1: Full time course of substrate disappearance as measured at 340 nm by stopped flow using wild type (wt) and mutants of DHFR. Enzyme (0.05 μM) was preincubated with 20 μM NADPH, and 10 μM H_2F was added to start the reaction. Experiments performed in 50 mM Bis-Tris buffer, pH 7.2, at 20 °C containing 1 mM DTE and 0.1 mM EDTA.

(3 mM folic acid) to be eluted from the affinity resin.

Enzyme Activity. Specific activities were determined for the wild-type and mutant enzymes as measured from the initial portion of a full time course in the presence of 20 μM NADPH and 10 μM H_2F using 0.05 μM enzyme. In order to avoid hysteretic effects (Penner & Frieden, 1985), the enzyme was preincubated with NADPH. Figure 1 shows these full time courses for the three mutants and wild-type protein. Previous kinetic experiments have shown that the Michaelis constants are considerably less than 1 μM (Fierke et al., 1987; Penner & Frieden, 1987) and that the curvature in these progress curves is a consequence of the formation of abortive complexes, with the dissociation of H_4F from either the complex or the free enzyme as limiting steps in the reaction. A comparison of the curves in Figure 1 indicates that the full time courses for the three mutants and wild-type protein all show the same curvature as a function of time. The results imply that the kinetic mechanism is unchanged in the three mutants. Specific velocities obtained from the initial portion of these curves show that under these conditions the valine deletion mutant is most active (v_0 = 16.5 s^{-1}) while the isoleucine and alanine mutants are somewhat more active (9.6 and 7.5 s^{-1}, respectively) than the wild-type enzyme (7.0 s^{-1}).

Substrate Quenching of Native Protein Fluorescence. As has been previously observed, formation of the binary DHFR–NADPH or DHFR–H_2F binary complex is a multiphase process with the fast phase reflecting the binding step and the slower portion of the fluorescence change reflecting the conversion of a less active (or less tightly binding) form of the enzyme to the active (or more tightly binding) form (Cayley et al., 1981; Penner & Frieden, 1987). Experiments were performed using either 2 μM H_2folate or 5 μM NADPH for the native protein and the three mutants. In all cases, the results for the mutant proteins were similar to those for the native enzyme. The apparent rate constant for the slow phase (reflecting interconversion of forms) ranged from 0.02 to 0.03 s^{-1} whether NADPH or H_2F was used for wild type and mutants. The percentage of all mutants and wild-type enzyme in the active form under these conditions was 60% using NADPH and 40–50% using H_2F. This type of difference between NADPH and H_2F has been observed previously (Penner & Frieden, 1987). The data indicate little or no changes in the ratio of the active to less active form or in the rate of conversion of the less active to active form for mutants compared to wild-type DHFR.

Table I: Urea Equilibrium Unfolding Parameters[a]

DHFR	θ_N[b] (mdeg)	m_N[b] (M^{-1})	θ_U[b] (mdeg)	m_U[b] (M^{-1})	ΔG_{H_2O}[b] (kcal/mol)	m_G[b] [kcal/(mol·M)]	$[urea]_{1/2}$[b] (M)	$\Delta\Delta G°$[b] (kcal/mol)
wtDHFR	−7.31 ± 0.07	0[c]	−2.27 ± 0.08	0	5.16 ± 0.12	−1.56 ± 0.12	3.30	0.0
ΔVal88	−7.01 ± 0.08	0.40 ± 0.15	−3.84 ± 0.20	0.27 ± 0.47	4.67 ± 0.78	−2.51 ± 0.39	1.86	2.93 ± 0.60
V88A	−7.74 ± 0.05	0	−2.09 ± 0.67	0.12 ± 0.10	5.55 ± 0.34	−1.62 ± 0.11	3.43	−0.20 ± 0.02
V88I	−7.51 ± 0.07	0	−3.15 ± 0.30	0.30 ± 0.06	5.91 ± 0.50	−2.44 ± 0.20	2.42	1.73 ± 0.20

[a] All solutions contained 20 mM phosphate and 0.1 mM EDTA adjusted to pH 7.2 at 20 °C. [b] θ_N and θ_U are the values for the molar ellipticity at 222 nm for the native and unfolded protein extrapolated to 0 M urea, respectively. m_N and m_U are the slope terms describing the dependence of θ_N and θ_U on urea concentration. ΔG_{H_2O} is the apparent free energy difference between the folded and unfolded forms of the protein extrapolated to 0 M urea. m_G is the slope describing the dependence of ΔG on denaturant concentration. $[urea]_{1/2}$ is the urea concentration at the midpoint of the transition. $\Delta\Delta G_U$ was calculated from the equation $\Delta\Delta G_U = 0.5[m_G(wt) + m_G(mut)][urea]_{1/2}$ (Kellis et al., 1989). [c] The fitted value of this parameter under these conditions was not significantly different from 0.

Table II: Rate Constants for Refolding from Urea

	20 °C				10 °C			
	k_1[a]	k_2	k_3	k_4	k_1	k_2	k_3	k_4
wt[b]	6.6	2.3	0.3	0.033	2.6	0.87	0.14	0.011
V88A[c]	6.9	2.3	0.17	0.037	2.7	0.87	0.13	0.013
V88I[d]	7.3	1.1	0.28	0.032	3.0	0.33	0.10	0.011
ΔV88[e]	10.0	0.75	0.1	0.028	3.8	0.35	0.13	0.011

[a] All rate constants in s^{-1} with errors of ±10%. [b] Determined from the dilution of a 4.5 M urea solution containing 0.1 mg/mL (5.5 μM) wtDHFR in 0.02 M phosphate buffer, pH 7.2, containing 1 mM DTE and 0.1 mM EDTA. [c] Determined from the dilution of a 4.6 M urea solution containing 0.1 mg/mL enzyme to 1.31 M urea in phosphate buffer. [d] Determined from the dilution of a 3.6 M urea solution containing 0.1 mg/mL enzyme to 1.03 M urea in phosphate buffer. [e] Determined from the dilution of a 3.06 M urea solution containing 0.1 mg/mL enzyme to 0.87 M urea in phosphate buffer.

Equilibrium Studies. A summary of the equilibrium data for the folding/unfolding process of the wild-type and mutant proteins is given in Table I. The equilibrium unfolding curves for the wild-type and mutant enzymes (Figure 2) represent a cooperative, two-state model for denaturation. The data provided a good fit to the mathematical expression of a two-state process (see eq 1), and it would appear that there are no stable intermediates in the equilibrium unfolding curve. The urea concentration at the midpoint of the unfolding transition is used for comparison of stabilities of wild-type and mutant DHFR proteins, since the error associated with this value is much less than the ΔG_{H_2O} values, which are extrapolated back to 0 M urea.

The midpoint for unfolding of the wild-type protein is at 3.30 M urea, in agreement with previously reported values (Touchette et al., 1986). The unfolding midpoint for the ΔV88 deletion mutant, 1.86 M urea, is significantly lower than for the wild-type protein and lower than for any other DHFR folding mutant published. The midpoint for the V88A mutant is 3.42 M urea. The small increase in the unfolding midpoint from 3.30 M urea for the wild-type DHFR represents a slight stabilization resulting from the alanine substitution. Substitution of valine-88 with isoleucine destabilizes the protein, as reflected by the unfolding midpoint of 2.4 M urea. This value is between the midpoints of the wild-type DHFR protein and the ΔV88 mutant. The values for $\Delta\Delta G$ were calculated from the equation (Kellis et al., 1989):

$$\Delta\Delta G_U = 0.5(m_{wt} + m_{mut})\Delta[urea]_{50\%}$$

Kinetic Refolding Studies. As first observed by Touchette et al. (1986), fluorescence changes on refolding DHFR from high urea concentrations first show an increase in fluorescence and then a fluorescence decrease characterized by three additional processes. These authors also observed that the rate constants for the refolding process are dependent on the final urea concentration. In order to make experiments with the wild-type and mutant enzymes equivalent, we chose to make the initial urea concentrations 1.2 M above the midpoint of the urea folding/unfolding equilibrium curve for each mutant with a 3.5-fold dilution of the urea for initiating refolding (see Figure 2 and Table I). Thus, the initial and final urea concentrations used were 4.5 and 1.29, 4.65 and 1.31, 3.6 and 1.03, and 3.06 and 0.87 M for the wild-type, V88A, V88I, and ΔV88 mutants, respectively. The validity of this procedure is indicated by the data in Table II which show that the rate constants for the last two phases (k_3 and k_4) (at 10 °C) and the last phase (at 20 °C) are essentially the same in all cases. The striking observation is that at 10 °C the rate constant for the second phase is decreased over 2.5-fold for the V88I and ΔV88 mutants but is not affected in the V88A mutant. At 20 °C, the result is similar except that the rate constant for the third phase is decreased as well in the ΔV88 mutant. Additionally, the rate constant for the first phase in the ΔV88 mutant is increased about 50% at either 10 or 20 °C relative to wild type. Results shown in Table II are at both 20 and 10 °C since 10 °C was the condition previously used (Frieden, 1990) to show the sequential binding of substrates during refolding while 20 °C is the temperature used for most experiments reported here.

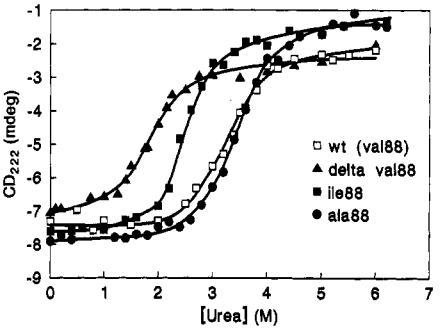

FIGURE 2: Equilibrium unfolding of *E. coli* wtDHFR (open squares), ΔV88 (filled triangles), V88A (filled circles), and V88I (filled squares) monitoring the urea-induced unfolding by the molar ellipticity at 222 nm. Each data point for the equilibrium curve consisted of 0.100 mg/mL DHFR protein, 0–6.0 M urea, 20 mM potassium phosphate, pH 7.2, and 0.1 mM EDTA. Samples were allowed to equilibrate 10 min at 20 °C in the water-jacketed cell in the spectrophotometer before data were collected.

Discussion

Figure 3 is a stereo representation of the apo form of *E. coli* dihydrofolate reductase. The region of interest in this study

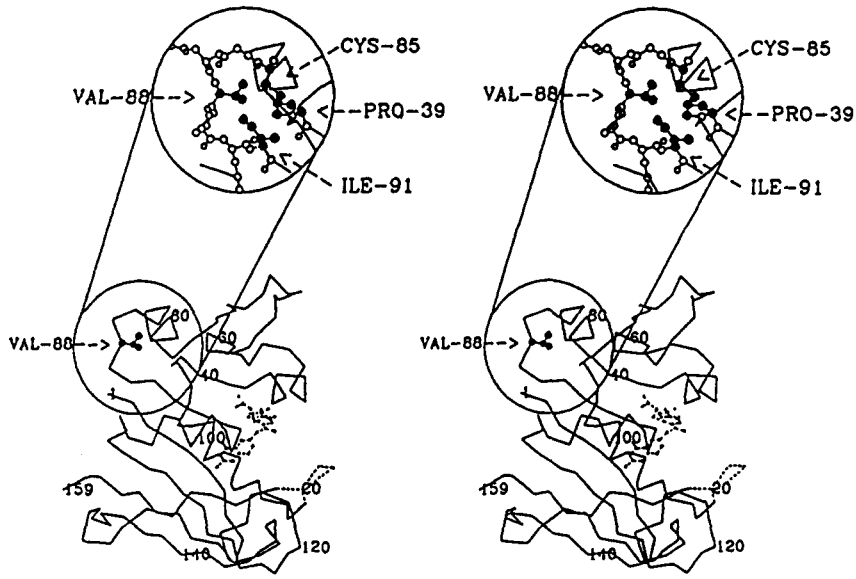

FIGURE 3: Stereo representation of the apo-DHFR structure (Bystroff & Kraut, 1991). The stereodiagram shows a C^{α}-model of apo-DHFR, based on the atomic coordinates deposited with code ID 5DFR in the Brookhaven Protein Data Bank (Bernstein et al., 1977). Residue numbers for every 20th residue are marked at the right of the C^{α}-atom. The side chain of Val88 is labeled and shown as filled circles. In order to indicate the approximate position of residues 16–20 in the apo-DHFR, the corresponding residues from the MXT–DHFR complex, BNL-Code 4DFR, have been included as stipled lines. The location of the methotrexate from the MXT–DHFR complex has also been marked with stipled lines. The zoomed enlargement shows all atoms in residues 85–91 as well as the side chains of Pro39, Cys85, Val88, and Ile91. These are shown as filled circles, and their locations are marked with arrows and labels. The stereodiagram was produced by the computer program ARPLOT of Lesk and Hardman (1982, 1985).

is the solvent-exposed loop shown in the inset. Valine-88, the central residue of the turn, points inwards toward the protein and forms a compact hydrophobic packing element by maintaining hydrophobic contacts with two other residues in the turn region, Cys-85 and Ile-91 as well as Pro-39. The ends of the loop that serve as connecting elements of secondary structure are not spatially proximal but are at right angles to each other and span across a hemisphere of the protein. The discussion below describes how the stability, enzymatic activity, and refolding properties of the enzyme may relate to the flexibility of this turn region.

Equilibrium Folding. It is clear that point mutations perturbing hydrophobic interactions in a solvent-exposed loop segment of *E. coli* DHFR can produce large changes in stability toward urea denaturation. The 85–91 loop is tightly packed with a congruent van der Waals surface that protrudes from the protein's surface when the wild-type *E. coli* DHFR structure (Bolin et al., 1982) is modeled on a Silicon Graphics Personal Iris. Using simple model-building procedures, we have made some estimates of the consequences of either deleting the valine-88 residue or replacing it with alanine or isoleucine. The V88A and V88I structures were constructed by replacing the valine-88 side chain with the alanine or isoleucine side chain, leaving the conformation of the backbone of residue 88 unchanged. The alanine and isoleucine side chains were "superimposed" on the valine-88 side chain to keep the orientation of the functional group of the amino acid facing inward toward the loop interior the same. The ΔV88 mutant was constructed by first deleting the valine residue entirely. The carboxy terminus of Asp87 was then joined to the amino terminus of Pro89. All mutant structures were subjected to 50 cycles of refinement in which the stereochemistry was regularized, and minor adjustments in ϕ and ψ angles of the peptide backbone were made to relieve any steric constraints introduced by the mutations. The coordinates of the α-carbon atoms of Cys85 and Ile91 were fixed to allow only the residues within the loop to adjust conformation during the refinement. Deletion of the valine-88 residue perturbed the van der Waals surface of the loop significantly and created an obvious cavity in the interior of the truncated loop. The deletion could be accommodated without requiring major changes in the rest of the molecule.

The packing of hydrophobic side chains in protein interiors is known to be an important determinant of their three-dimensional structure (Kellis et al., 1989; Dill, 1990) and stability (Matsumura et al., 1989; Sandberg & Terwilliger, 1989). In those studies, however, these packing interactions occur at residues buried between β-strands and/or α-helices, and were not described for turn residues since such residues appear almost exclusively at the surface of the protein. For DHFR, removing the valine-88 residue from the 85–91 loop interior destabilized the protein by 2.93 kcal/mol, the energetic cost expected when removing a hydrophobic side chain from the tightly packed hydrophobic core of a protein (Kellis et al., 1989; Sandberg & Terwilliger, 1989). These results suggested that the change in hydrophobic interactions in the valine-88 loop region could be responsible for the large destabilization of the ΔV88 mutant.

The results from the urea equilibrium experiments of the ΔV88, V88A, and V88I mutants, however, show no direct correlation between side-chain volume and stability. The alanine side chain of a single methyl group is much smaller than the valine side chain, yet the midpoint for unfolding this mutant was at 3.4 M urea, *more* stable than the wild-type protein by 0.20 kcal/mol. This result was extremely puzzling since deletion of the valine-88 side chain destabilized the protein drastically, and reducing the hydrophobic side-chain volume in the loop interior with the alanine substitution was also expected to destabilize the protein. The question of hydrophobic packing in the Ala88-substituted loop may have been complicated by the loop's flexibility. The smaller alanine substitution might not destabilize the protein if the loop could be reshuffled around the mutant site to optimize the packing in that region.

Substituting isoleucine for valine-88 destabilized the protein by 1.73 kcal/mol, lowering the unfolding transition midpoint

of the V88I mutant to 2.45 M urea. It seems reasonable to assume that the destabilization by the Ile88 substitution results from the larger hydrophobic side chain of isoleucine overcrowding the loop. Preliminary crystallographic data of the binary MTX complex indicate that there are slight differences between the wtDHFR and the V88I mutant (V. Nienaber, C. Kelly, and J. Birktoft, personal communication).

Mutations that restrict the loop's flexibility or function as a spacer element could destabilize the protein by producing unfavorable interactions such as misalignment of interacting regions of secondary structure or too close contacts between residues. It is possible that the deletion of valine-88, the central residue of the irregular loop, severely reduced the flexibility of the loop due to the limited conformations available to Pro89. Curiously, none of the mutations appear to markedly affect the turn's ability to act as a hinge or a mobile element of the protein for ligand-induced conformational changes or those that occur during catalysis (Penner & Frieden, 1985).

Enzyme Activity. The effects of the mutations at valine-88 on the activity of the enzyme are unclear since the valine-88 loop is at the surface of the protein away from the active-site region. One explanation is that perturbing the interactions within the valine-88 loop has long-range effects on the protein's conformation. Loop 85–91 acts as a connecting element between α-helix E and β-strand E. The carboxyl end of βE forms a tight turn that involves a cis peptide bond between Gly95 and Gly96 that overhangs the methotrexate binding pocket. The carbonyl oxygen of Ile94, which forms a parallel β-bulge with Gly95, hydrogen-bonds to N4 of methotrexate in the MTX–DHFR crystal structure and is proposed to hydrogen-bond with N8 of the dihydrofolate pteridine ring (Bystroff et al., 1990). Loop 85–91 may be involved in maintaining β-E in the correct orientation so that Ile94 is positioned correctly for hydrogen bonding with methotrexate (or the dihydrofolate substrate).

As indicated by Figure 1, it seems unlikely that differences in specific activity are due to changes in Michaelis constants for the substrate. First, the substrate concentrations used to determine the relative specific activities (10 and 20 μM for H_2F and NADPH, respectively) are well above the Michaelis constants for the wild-type enzyme (<1 μM). Larger K_m values for the mutants would only decrease the velocity relative to the wild type. Second, the full time courses for wild type and all mutants show similar behavior, indicating no major changes in the kinetic mechanism. Since the main rate-limiting process is the release of H_4F from the E–NADPH–H_2F complex, it is presumably this step that is affected. Differences in the flexibility of the valine-88 loop could facilitate this process by allowing movements in the β-E strand and the turn overhanging MTX in the active site. If mutations in this loop are perturbing motions of the protein affecting H_4F release, the activity would be altered.

For the V88A mutant, which has about the same specific activity (and stability) as the wild type, the flexibility of the loop may be unaffected, and substrate release appears essentially unchanged. The somewhat higher activity of the V88I mutant, which is less stable than wild type, may be a consequence of the overcrowding of the loop by the larger side chain, allowing an open configuration and H_4F release to occur more readily.

The ΔV88 enzyme is most interesting, since its activity is more than twice the specific activity of wtDHFR. Again, the most likely explanation is that the valine-88 deletion has significantly disturbed interactions within the loop and has altered its flexibility such that H_4F is released from the enzyme more efficiently and the activity increases accordingly. Deleting valine-88 shortens the connecting element to β-strand E by one residue, and may cause the loop overhanging the MTX binding pocket to be pulled away from the pocket. It is of interest that so far, we have been unable to grow crystals of the ΔV88 deletion mutant although such crystals can be obtained for the alanine and isoleucine mutants (J. Birktoft, personal communication).

The valine-88 loop is the site of variations in the enzyme's structure in different organisms. The analogous turn in *Lactobacillus casei* DHFR (Bolin et al., 1982) contains a two amino acid insertion that extends the α-helix E an additional half-turn before leading directly into β-sheet E, instead of the chain reversal accomplished by the loose *E. coli* 85–91 turn. The avian (Volz et al., 1982) and human (Oefner et al., 1988; Davies et al., 1990) DHFR structures both have large amino acid insertions at the *E. coli* 35–38 and 85–91 turns, the same "hinge" region targeted in these experiments. The human and *E. coli* DHFR proteins are structurally homologous, and there is a hinge region in the *E. coli* protein, residues 35–40, which might also be important in stability or folding properties. Mutagenesis experiments deleting two residues (Gly45 and Lys46) from a flexible loop region of human DHFR (Tan et al., 1990) analogous to the 35–38 turn of the *E. coli* structure suggest that the flexibility of this turn in the human DHFR structure is important for ligand-induced conformational changes and the catalytic efficiency of the enzyme. Tan et al. (1990) showed that deletion of the two residues eliminated the activation by KCl, urea, and organomercurials normally observed in the wild-type human DHFR enzyme, indicating differences in unfolding of the protein during activation.

Kinetics of Refolding. Five refolding phases have been previously reported for wtDHFR (Touchette et al., 1986) and mutant DHFR proteins (Garvey & Matthews, 1989). The slowest refolding phase with relaxation times of 300–1000 s was detected by using manual mixing techniques with difference UV spectroscopy. This phase has not been observed in this laboratory and is not considered to be associated with recovery of active enzyme (Frieden, 1990), and its identity as a folding event is uncertain. Thus, our experiments are described in terms of the four phases observed as changes in intrinsic fluorescence on refolding. All the mutant enzymes show the four phases observed for the wild type, but as shown in Table II, some of the rate constants differ. Presumably, the refolding pathway has not been altered. The rate constant for the first phase (k_1) is somewhat faster for the ΔV88 mutant than for the other mutants or the wild type. This phase has been attributed to burying Trp74 in a hydrophobic pocket (Garvey & Matthews, 1989; Garvey et al., 1989). If this interpretation is correct, it is possible that the deletion of the valine alters the rate of collapse of the hydrophobic region surrounding Trp74 during refolding.

A much larger, probably more significant, change in rate constants is associated with the second phase of refolding. It is this phase that has been proposed to create the H_2F binding site during refolding (Frieden, 1990). In both the ΔV88 and V88I mutants, the rate constant is decreased over 2.5-fold. Interestingly, the rate constant for the fourth phase, that associated with the formation of the NADP(H) site (Frieden, 1990), is the same in all the mutants and equal to that of the wild type under the conditions used in these experiments. As noted earlier, the rate constants for the refolding process are dependent on the final urea concentration (Touchette et al., 1986). Indeed, that is also true of the mutant enzymes used in this study (data not shown). If we use the rate constant

of the final phase as a "marker" and if it is the same in all cases, then the rate constants for the other phases can be considered as relative values between wild type and mutants. In this sense, the observation that the rate constant for the second phase is decreased is significant.

The valine-88 loop is a pivot point in the DHFR structure for the movement of a domainlike segment of the protein structure inward toward the MTX binding pocket (Bolin et al., 1982; Bystroff & Kraut, 1991) during MTX binding by the apoenzyme. We have shown that mutations which perturb the flexibility of the valine-88 hinge region (ΔV88 and V88I) have substantial effects on the stability and the activity of DHFR. We think, therefore, it possible that the valine-88 loop is also acting as a hinge or a flexible element in the folding process.

As noted above, the second refolding phase that has been associated with H_2F binding (and, therefore, the formation of a binding pocket for H_2F) is much slower for the ΔV88 and V88I mutants. Since these mutants show the largest perturbations in stability and enzymatic activity, it is reasonable that the second refolding phase is slowed due to a decreased flexibility of the valine-88 hinge region. Thus, the hinge region responsible for stability and activity changes of the protein may also act as a hinge in the folding process. The valine-88 loop most likely acts as a pivot point to bring together preformed elements of the DHFR protein to form the active-site region (and allow H_2F binding) during this phase of the refolding process detected by fluorescence.

In summary, the interaction of hydrophobic residues in the interior of the solvent-exposed valine-88 loop of *E. coli* DHFR has a surprising effect on the stability, activity, and refolding properties of the protein. The effects of the mutations are possibly due to changing the loop's function as a spacer element to position the connecting β-strand over the active-site pocket. Many folding studies have focused on the association of α-helices and β-sheets during the folding process, but the data in this paper imply that the turn or loop regions provide the conformational flexibility for these tertiary contacts to be established.

Acknowledgments

We are grateful to Dr. Jens Birktoft for many helpful discussions and for providing graphics and preliminary crystallographic data and to Sheryl Stafford for technical assistance.

References

Ahrweiler, P. M., & Frieden, C. (1988) *J. Bacteriol. 170*, 3301–3304.

Alber, T., Dao-pin, S., Wilson, K., Wozniak, J. A., Cook, S. P., & Matthews, B. (1987) *Nature 330*, 41–46.

Baccanari, D., Phillips, A., Smith, S., Sinski, D., & Burchall, J. (1975) *Biochemistry 14*, 5267–5273.

Bernstein, F. C., Koetzle, T. F., Williams, G. J. B., Meyer, E. F., Jr., Brice, M. D., Rodgers, J. R., Kennard, O., Shimanouchi, T., & Tasumi, M. (1977) *J. Mol. Biol. 112*, 535–542.

Bolin, J. J., Filman, D. J., Matthews, D. A., Hamlin, R. C., & Kraut, J. (1982) *J. Biol. Chem. 257*, 13650–13662.

Bystroff, C., & Kraut, J. (1991) *Biochemistry 30*, 2227–2239.

Bystroff, C., Oatley, S. J., & Kraut, J. (1990) *Biochemistry 29*, 3263–3277.

Cameron, J. R., Loh, E. Y., & Davis, R. W. (1979) *Cell 16*, 739–751.

Cayley, P. J., Dunn, S. M. J., & King, R. W. (1981) *Biochemistry 20*, 874–879.

Davies, J. F., Delcamp, T. J., Prendergast, N. J., Ashford, V. A., Freisheim, J. H., & Kraut, J. (1990) *Biochemistry 29*, 9467–9479.

Dill, K. A. (1990) *Biochemistry 29*, 7133–7155.

Dunn, S. M. J., Lanigan, T. M., & Howell, E. E. (1990) *Biochemistry 29*, 8569–8576.

Fierke, C. A., Johnson, K. A., & Benkovic, S. J. (1987) *Biochemistry 26*, 4085–4092.

Filman, D. J., Bolin, J. T., Matthews, D. A., Hamlin, R. C., & Kraut, J. (1982) *J. Biol. Chem. 257*, 13363.

Frieden, C. (1990) *Proc. Natl. Acad. Sci. U.S.A. 87*, 4413–4416.

Garvey, E. P., & Matthews, C. R. (1989) *Biochemistry 28*, 2083–2093.

Garvey, E. P., Swank, J., & Matthews, C. R. (1989) *Proteins: Struct., Funct., Genet. 6*, 259–266.

Hynes, T. R., Kautz, R. A., Goodman, M. A., Gill, J. F., & Fox, R. O. (1989) *Nature 339*, 73–76.

Kellis, J. T., Jr., Nyberg, K., Sali, D., & Fersht, A. (1988) *Nature 333*, 784–786.

Lesk, A. M., & Hardman, K. D. (1982) *Science 216*, 539–540.

Lesk, A. M., & Hardman, K. D. (1985) *Methods Enzymol. 115*, 381–390.

Leszczynski, J. F., & Rose, G. D. (1987) *J. Biol. Chem. 234*, 849–855.

Maniatis, T., Fritsch, E. F., & Sambrook, J. (1982) *Molecular Cloning: a laboratory manual*, Cold Spring Harbor Laboratory, Cold Spring Harbor, NY.

Matsumura, M., Wozniak, J. A., Dao-pin, S., & Matthews, B. W. (1989) *J. Biol. Chem. 264*, 16059–16066.

Miller, J. H. (1977) *Experiments in Molecular Genetics*, Cold Spring Harbor Laboratory Publications, Cold Spring Harbor, NY.

Oefner, C., D'Arcy, A., & Winkler, F. K. (1988) *Eur. J. Biochem. 174*, 377–385.

Pace, C. N. (1986) *Methods Enzymol. 131*, 266–280.

Pain, R. (1987) *Trends Biol. Sci. 12*, 309–312.

Penner, M. H., & Frieden, C. (1985) *J. Biol. Chem. 260*, 5366–5368.

Penner, M. H., & Frieden, C. (1987) *J. Biol. Chem. 262*, 15908–15914.

Perry, K. M., Onuffer, J. J., Touchette, N. A., Herndon, C. S., Gittelman, M. S., Matthews, C. R., Chen, J.-T., Mayer, R. J., Tiara, K., Benkovic, S. J., Howell, E. E., & Kraut, J. (1987) *Biochemistry 26*, 2674–2682.

Perry, K. M., Onuffer, J. J., Gittelman, M. S., Barmat, L., & Matthews, C. R. (1989) *Biochemistry 28*, 7961–7968.

Prendergast, N. J., Delcamp, T. J., Smith, P. L., & Freisheim, J. H. (1988) *Biochemistry 27*, 3664–3671.

Santoro, M. M., & Bolen, D. W. (1988) *Biochemistry 27*, 8063–8068.

Skolnick, J., & Kolinski, A. (1990) *Science 250*, 1121–1125.

Stone, S. R., & Morrison, J. F. (1982) *Biochemistry 21*, 3757–3765.

Syberg, W. S., & Terwilliger, T. C. (1989) *Science 245*, 54–57.

Tan, X., Huang, S., Ratnam, M., Thompson, P. D., & Freisheim, J. H. (1990) *J. Biol. Chem. 265*, 8027–8032.

Touchette, N. A., Perry, K. M., & Matthews, C. R. (1986) *Biochemistry 25*, 5445–5452.

Vanderyar, M., Weiner, M., Hutton, C., & Batt, C. (1988) *Gene 65*, 129–133.

Villafranca, J. E., Howell, E. E., Voet, D. H., Strobel, M. J., Ogden, R. C., Abelson, J. N., & Kraut, J. (1983) *Science 222*, 782–788.
Volz, K. W., Matthews, D. A., Alden, R. A., Freer, S. T., Hansch, C., Kaufman, B. T., & Kraut, J. (1982) *J. Biol. Chem. 257*, 2528–2536.
Wallace, C. J. A. (1987) *J. Biol. Chem. 262*, 16767–16770.
Williams, J. W., Morrison, J. F., & Duggleby, R. G. (1979) *Biochemistry 18*, 2567–2573.
Zakrzewski, S. F., & Sansone, A. M. (1971) *Methods Enzymol. 18B*, 728–731.
Zoller, M. J., & Smith (1972) *Nucleic Acids Res. 10*, 6487.

A Mammalian Tryptophanyl-tRNA Synthetase Shows Little Homology to Prokaryotic Synthetases but Near Identity with Mammalian Peptide Chain Release Factor[†,‡]

Maurice Garret,[§] Bertrand Pajot,[§] Véronique Trézéguet,[§] Julie Labouesse,[§] Michel Merle,[§] Jean-Claude Gandar,[§] Jean-Pierre Benedetto,[§] Marie-Line Sallafranque,[§] Jeanine Alterio,[∥] Maryse Gueguen,[§] Claude Sarger,[§] Bernard Labouesse,[§] and Jacques Bonnet*[,§]

Institut de Biochimie Cellulaire et Neurochimie du CNRS, Université de Bordeaux II, 1 rue Camille Saint-Saëns, 33077 Bordeaux Cedex, France, and INSERM U 118, 29 rue Wilhem, Paris, France

Received December 3, 1990; Revised Manuscript Received May 3, 1991

ABSTRACT: Determination of the amino acid sequence of beef pancreas tryptophanyl-tRNA synthetase was undertaken through both cDNA and direct peptide sequencing. A full-length cDNA clone containing a 475 amino acid open reading frame was obtained. The molecular mass of the corresponding peptide chain, 53 728 Da, was in agreement with that of beef tryptophanyl-tRNA synthetase, as determined by physicochemical methods (54 kDa). Expression of this clone in *Escherichia coli* led to tryptophanyl-tRNA synthetase activity in cell extracts. The open reading frame included two sequences analogous to the consensus sequences, HIGH and KMSKS, found in class I aminoacyl-tRNA synthetases. The homology with prokaryotic and yeast mitochondrial tryptophanyl-tRNA synthetases was low and was limited to the regions of the consensus sequences. However, a 90% homology was observed with the recently described rabbit peptide chain release factor (eRF) [Lee et al. (1990) *Proc. Natl. Acad. Sci. 87*, 3508–3512]. Such a strong homology may reveal a new group of genes deriving from a common ancestor, the products of which could be involved in tRNA aminoacylation (tryptophanyl-tRNA synthetase) or translation termination (eRF).

Besides their primary role in tRNA aminoacylation, aminoacyl-tRNA synthetases exhibit in vivo complementary functions such as splicing of mitochondrial RNAs in *Neurospora crassa* or yeast (Atkins & Lambovitz, 1982; Herbert et al., 1986) and regulation of translation initiation (Clemens, 1990). They also exhibit in vitro several catalytic activities which are the consequence of their ability to synthesize a highly reactive aminoacyl adenylate (Weiss et al., 1959; Tada & Tada, 1975; Plateau et al., 1981; Lorber et al., 1982; Andrews et al., 1985). Complementary functions or properties may be expected in eukaryotes, because cytoplasmic aminoacyl-tRNA synthetases are larger in size than their prokaryotic counterparts (Schimmel & Söll, 1979; Schimmel, 1987). For example, eight to ten eukaryotic aminoacyl-tRNA synthetases can be purified as high molecular weight multienzyme complexes (Dang et al., 1982; Cirakoglu & Waller, 1986) while prokaryotic synthetases cannot. Beef tryptophanyl-tRNA synthetase (WRS), however, has never been found in such complexes (Bec et al., 1989), although its molecular weight is higher than that of prokaryotic ones [54 kDa as compared to 37 kDa for the *Bacillus stearothermophilus* protein (Winter & Hartley, 1977)]. Beef WRS presents another noticeable feature: its concentration is 2 orders of magnitude larger in pancreas than in other organs (Sallafranque et al., 1986; Favorova et al., 1989), amounting to around 1% of the total protein concentration of this gland. This amount by far exceeds what is necessary for protein biosynthesis. Furthermore, in beef pancreas, its activity is much higher than that of the other aminoacyl-tRNA synthetases (Davie et al., 1956).

The catalytic properties of beef WRS have been extensively studied (Akhverdyan et al., 1977; Trézéguet et al., 1986; Merle et al., 1988) but have not been related to its molecular structure, which to date has not been described. Up to now, very few aminoacyl-tRNA synthetases of higher eukaryotes have been sequenced and the three-dimensional structure of none has been solved. Therefore, further insight into the molecular properties of these enzymes requires better knowledge of their structures. To obtain such information, the determination of the amino acid sequence of beef WRS was undertaken through both cDNA cloning and direct peptide sequencing. Very unexpectedly, this sequence turned out to be nearly identical with that of the eukaryotic peptide release factor (Lee et al., 1990).

Materials and Methods

Materials

Radionucleotides were from Amersham Corp. Restriction and modifying enzymes and chemicals were from BRL, Boehringer, Pierce, and Sigma. They were of the highest

[†] Supported by grants from the CNRS, the Université de Bordeaux II, and the Région Aquitaine.
[‡] The full cDNA sequence in this paper has been submitted to the EMBL Data Bank under Accession Number X 53918 and to GenBank under Accession Number J05334.
[§] Université de Bordeaux II.
[∥] INSERM U 118.

0006-2960/91/0430-7809$02.50/0